

STELLAR POPULATIONS AT THE CENTER OF IC 1613¹

ANDREW A. COLE,² ELINE TOLSTOY,³ JOHN S. GALLAGHER, III,² JOHN G. HOESSEL,²
 JEREMY R. MOULD,⁴ JON A. HOLTZMAN,⁵ ABHIJIT SAHA,⁶ GILDA E. BALLESTER,⁷
 CHRISTOPHER J. BURROWS,^{8,9} JOHN T. CLARKE,⁷ DAVID CRISP,¹⁰ RICHARD E.
 GRIFFITHS,¹¹ CARL J. GRILLMAIR,¹² JEFF J. HESTER,¹³ JOHN E. KRIST,⁸ VIKKI
 MEADOWS,¹⁰ PAUL A. SCOWEN,¹³ KARL R. STAPELFELDT,¹⁰ JOHN T. TRAUGER,¹⁰
 ALAN M. WATSON,¹⁴ AND JAMES R. WESTPHAL¹⁵

Draft version August 28, 2018

ABSTRACT

We have observed the center of the Local Group dwarf irregular galaxy IC 1613 with WFPC2 aboard the *Hubble Space Telescope* in the F439W, F555W, and F814W filters. We analyze the resulting color-magnitude diagrams (CMDs) using the main-sequence and giant branch luminosity functions and comparisons to theoretical stellar models to derive a preliminary star-formation history for this galaxy. We find a dominant old stellar population (aged ≈ 7 Gyr), identifiable by the strong red giant branch (RGB) and red clump populations. From the (V-I) color of the RGB, we estimate a mean metallicity of the intermediate-age stellar population $[\text{Fe}/\text{H}] = -1.38 \pm 0.31$. We confirm a distance of 715 ± 40 kpc using the I-magnitude of the RGB tip. The main-sequence luminosity function down to $I \approx 25$ provides evidence for a roughly constant SFR of approximately $3.5 \times 10^{-4} M_{\odot} \text{ yr}^{-1}$ across the WFPC2 field of view (0.22 kpc^2) during the past 250–350 Myr. Structure in the blue loop luminosity function implies that the SFR was $\approx 50\%$ higher 400–900 Myr ago than today. The mean heavy element abundance of these young stars is $\approx 1/10$ solar. The best explanation for a red spur on the main-sequence at $I \approx 24.7$ is the blue horizontal branch component of a very old stellar population at the center of IC 1613. We have also imaged a broader area of IC 1613 using the 3.5-meter WIYN telescope under excellent seeing conditions. The WIYN color-magnitude diagram reveals a prominent sequence of asymptotic giant branch stars and red supergiants that is less prominent in the WFPC2 CMD due to the smaller field of view. The AGB-star luminosity function is consistent with a period of continuous star formation over at least the age range 2–10 Gyr. We present an approximate age-metallicity relation for IC 1613, which appears similar to that of the Small Magellanic Cloud. We compare the Hess diagram of IC 1613 to similar data for three other Local Group dwarf galaxies, and find that IC 1613 most closely resembles the nearby, transition-type dwarf galaxy Pegasus (DDO 216).

¹Based on observations made with the NASA/ESA *Hubble Space Telescope*, obtained at the Space Telescope Science Institute, which is operated by the Association of Universities for Research in Astronomy, Inc., under NASA contract NAS 5-26555, and with the WIYN telescope at the Kitt Peak National Observatory.

²Department of Astronomy, University of Wisconsin-Madison, 475 N. Charter Street, Madison, WI 53706; *cole@astro.wisc.edu*, *hoessel@astro.wisc.edu*, *jsg@tiger.astro.wisc.edu*.

³European Southern Observatory, Karl-Schwarzschild-Straße, Garching bei München, Germany; *etolstoy@eso.org*.

⁴Mt. Stromlo and Siding Spring Observatories, Australian National University, Private Bag, Weston Creek Post Office, ACT 2611, Australia.

⁵Department of Astronomy, New Mexico State University, Box 30001 Department 4500, Las Cruces, NM 88003-8001.

⁶National Optical Astronomy Observatories, 950 North Cherry Avenue, Tucson, AZ 85726.

⁷Department of Atmospheric and Oceanic Sciences, University of Michigan, 2455 Hayward, Ann Arbor, MI 48109.

⁸Space Telescope Science Institute, 3700 San Martin Drive, Baltimore, MD 21218.

⁹Astrophysics Division, Space Science Department, European Space Agency.

¹⁰Jet Propulsion Laboratory, 4800 Oak Grove Drive, Mail Stop 183-900, Pasadena, CA 91109.

¹¹Carnegie-Mellon University, Department of Physics, 5000 Forbes Avenue, Pittsburgh, PA 15213.

¹²SIRTF Science Center, California Institute of Technology, 770 South Wilson, Pasadena, CA 91125.

¹³Department of Physics and Astronomy, Arizona State University, Tyler Mall, Tempe, AZ 85287.

¹⁴Instituto de Astronomía UNAM, 58090 Morelia, Michoacan, Mexico.

¹⁵Division of Geological and Planetary Sciences, MS 170-25, California Institute of Technology, Pasadena, CA 91125.

Subject headings: galaxies: individual (IC 1613) — color-magnitude diagrams — galaxies: stellar content — Local Group — galaxies: irregular

1. INTRODUCTION

The study of stellar populations is a way for astronomers to explore galaxy evolution, providing direct information on the variations of star-formation rate and mean abundance with time, from the present-day back to the initial formation of a galaxy. The ensemble of Local Group dwarf galaxies, because of their diversity of sizes, environments, and chemical abundances makes a good laboratory in which to investigate the processes which control galaxy evolution (e.g., Hodge 1989; Da Costa 1998; Grebel 1998; Tolstoy 1999).

Dwarf galaxies are the most common class of galaxy in the Universe, but there are a number of unresolved questions of dwarf galaxy evolution; the relation between the early- (elliptical/spheroidal) and late- (irregular) type galaxies, the effects of environment on galaxy evolution, and the patterns of chemical enrichment are unanswered questions (Mateo 1998). Additionally, it may be that the ubiquitous faint, blue galaxies seen in redshift surveys (e.g. Ellis 1997) are the precursors of today's dwarf galaxies. The most straightforward way to trace this possible cosmological connection is by a determination of the star-formation histories of the nearby dwarf galaxies (Tolstoy 1998).

Color-magnitude diagrams which include one or more main-sequence turnoffs are a powerful tool for the determination of detailed star-formation histories for galaxies. However, stellar crowding at the level of the horizontal branch and below has made this task all but impossible for ground-based telescopes. Consequently, most studies to date have concentrated on the sparse, late-type dwarf galaxies, or the relatively uncrowded outer fields around dwarf irregulars. WFPC2 has made it possible to push stellar photometry down below the magnitude of the horizontal branch throughout the Local Group, opening new vistas for the study of stellar populations in dwarf irregular galaxies.

In a Cycle 6 Guaranteed Time Observer program, we obtained deep BVI images of IC 1613 (DDO 8), one of the charter members of the Local Group (Hubble 1936), in order to constrain the ages and metallicities of the stellar populations in this object. In this paper we present the WFPC2 VI color-magnitude diagram of IC 1613, complemented by ground-based images taken at the WIYN telescope.¹ Section 2 gives a summary of IC 1613's properties, and in section 3 we describe our observations and measurement pro-

cedures. Section 4 presents our color-magnitude diagrams of IC 1613, and the stellar populations analysis is given in section 5. We discuss IC 1613's range of metal abundance and relation to a sample of Local Group dwarfs for which WFPC2 stellar population studies have been made in section 6, and summarize our results in section 7.

2. IC 1613: BACKGROUND

IC 1613 was discovered by Wolf in 1906, who noted an extended grouping of faint nebulosities near the star 26 Ceti (Wolf 1907). IC 1613 was first resolved into stars, at magnitude 17–18, by Baade (1928), who identified it as a Magellanic Cloud-type galaxy and compared it to NGC 6822. IC 1613 was Baade's (1963) prime example of the eponymous sheet of Population II red giant stars that seem to exist in all Local Group dwarfs (Baade 1963; Sandage 1971b).

Due to low values of both foreground and internal reddening along IC 1613 sightlines, it has played an important role in the calibration of the Cepheid variable Period-Luminosity relation for the determination of extragalactic distances (Baade 1935, Sandage 1971a). IC 1613 is the *only* Local Group dwarf irregular galaxy, apart from the Magellanic Clouds, in which RR Lyrae type variables have been detected (Saha *et al.* 1992; Mateo 1998).

IC 1613 occupies a relatively isolated position in the Local Group, ≈ 400 kpc from M33, ≈ 500 kpc from M31, and ≈ 700 kpc from the Milky Way. Its known neighbors within 400 kpc are the comparably luminous WLM irregular (DDO 221), at ≈ 390 kpc, the smaller Pegasus dwarf (DDO 216), some 360 kpc distant, and the tiny ($M_V = -9.7$) Pisces dwarf (LGS 3), at ≈ 280 kpc distance. This minor quartet of galaxies share similar ranges of chemical abundance, and a roughly constant long-term star-formation rate. They show varying amounts of recent star formation, but each have stellar populations that in the mean are older than $\gtrsim 3$ Gyr (Pegasus—Gallagher *et al.* 1998; Pisces—Aparicio, Gallart & Bertelli 1997; WLM—Minniti & Zijlstra 1996; IC 1613—Freedman 1988a; this paper). Pegasus and Pisces have been classified as “transition” galaxies, intermediate between the irregular and spheroidal classes (Mateo 1998), although the significance of this distinction has been called into question (Aparicio *et al.* 1997). The newly discovered Andromeda VI (Pegasus dwarf spheroidal) also lies $\approx 400 \pm 40$ kpc from IC 1613 (Grebel & Guhathakurta 1999).

The basic parameters of IC 1613 are summarized in

¹The WIYN Observatory is a joint facility of the University of Wisconsin-Madison, Indiana University, Yale University, and the National Optical Astronomy Observatories.

TABLE 1
BASIC PROPERTIES OF IC 1613

Property	Value	Source
ℓ, b (2000.0)	129°8, -60°6	Mateo 1998
$(m-M)_0$	24.27 ± 0.10	Lee <i>et al.</i> 1993
E_{B-V}	0.03 ± 0.02	Mateo 1998
M_V	-15.2 ± 0.2	Hodge 1978
$B-V_0$	0.71 ± 0.1	Hodge 1978
$M(\text{HI}) (10^6 M_\odot)$	54 ± 11	Lake & Skillman 1989
$M(\text{HI})/L_B (M_\odot/L_\odot)$	0.81	Mateo 1998
R_{core} (arcsec) ^a	200:	Hodge <i>et al.</i> 1991
$L(\text{H}\alpha)$ (erg s ⁻¹)	3.18×10^{38}	Hunter <i>et al.</i> 1993
$SFR_0 (10^{-3} M_\odot/\text{yr})^b$	2.9 ± 0.7	this paper

^acore radius of best fit King model to unresolved light profile.

^bderived from extinction-corrected H α flux, see text.

Table 1. The distance is unusually secure due to the large number of Cepheid variables and low reddening towards IC 1613 (Sandage 1971a, Freedman 1988b); the RR Lyrae distance (Saha *et al.* 1992) and RGB tip distance (Freedman 1988a; Lee *et al.* 1993) are in agreement to within the errors. The reddening maps of Burstein & Heiles (1982) show $E_{B-V} \leq 0.03$ mag towards IC 1613; Freedman (1988a) derived $E_{B-V} = 0.04$. Recent work by Schlegel, Finkbeiner & Davis (1998) finds a foreground component $E_{B-V} = 0.01$.

We include the scale length of IC 1613's surface brightness profile in Table 1, to emphasize the fact that the WFPC2 field, $\approx 150''$ across, images only a small portion of the central galaxy. As Hodge *et al.* (1991) emphasize, the tabulated scale length is highly uncertain due to the low light levels, small number statistics, and the hard-to-define tradeoffs between model parameters.

The H α luminosity in Table 1 is taken from Hunter, Hawley, & Gallagher (1993), adjusted downwards to compensate for their assumed distance of 900 kpc to IC 1613. The H α luminosity of a galaxy provides a method to estimate the recent (0–10 Myr) star-formation rate. Hunter & Gallagher (1986) derive

$$\dot{M} = 7.07 \times 10^{-42} L(\text{H}\alpha) M_\odot \text{ yr}^{-1}, \quad (1)$$

with a possible additional factor of ~ 1.6 to be added to account for internal extinction within their sample of calibrating galaxies. We find a total star-formation rate over the past 10 Myr of $2.9 \pm 0.7 \times 10^{-3} M_\odot \text{ yr}^{-1}$ for IC 1613.

3. THE DATA

3.1. Observations & Reductions

IC 1613 was observed with WFPC2 over 9 orbits on 26–27 August, 1997. The PC chip was centered 97'' southwest of the center of the galaxy, at right ascension 1^h 04^m 48^s.7, declination +02° 07' 06''.2 (J2000.0). Exposures totalling 10,700 sec each were taken through the F555W (WFPC2 V) and F814W (WFPC2 I) filters. F439W (WFPC2 B) images totalling 2,600 sec were also obtained. The short, blue exposures were intended to provide photometry of the younger, more luminous main-sequence and blue loop stars. The images are available online at the HST Data Archive under the listing for Program ID# 6865.

All images were reduced using the standard pipeline at the Space Telescope Science Institute (Holtzman *et al.* 1995a), and combined using a cosmic-ray cleaning algorithm. The combined F555W image is shown in Figure 1. The field of view was oriented to place the center of IC 1613 in the WF3 chip; most of the central H I hole (Skillman 1987; Lake & Skillman 1989) is contained within the five square-arcminute field. Additionally, the field was chosen to avoid H II regions (Hodge, Lee & Gurnwell 1990) in order to focus attention on the older main-sequence stars that cannot be photometered from the ground due to crowding. The low stellar and gas density of IC 1613 are clearly evident by the clarity with which background galaxies can be seen.

Figure 1
can be obtained from
the following URL:

<http://www.astro.wisc.edu/~cole/ic1613.fig1.eps>

FIG. 1.— WFPC2 F555W image of the center of IC 1613. North and East are as marked; the field of view is roughly 3'5 across the widest corner-to-corner span. The low stellar density of IC 1613 is highlighted by the large number of background galaxies in the image.

3.2. Photometry

We performed profile-fitting photometry on our reduced, combined images using the DoPHOT routines and techniques described in Schechter, Mateo and Saha (1993); the code has been modified to handle the complexities of the WFPC2 point spread function (Saha *et al.* 1994). Using the DoPHOT star-matching routines, we identified 47,263 stars in both the F555W and F814W frames; the shallower F439W exposures permitted the cross-identification of just 7,922 stars in the F439W and F555W images. Our data have limiting magnitudes for photometry of $V \sim 26.5$, $I \sim 25.5$, and $B \sim 25$.

We transformed our photometry to the Johnson-Cousins BVI system by making aperture corrections to the 0'5 aperture recommended by Holtzman *et al.* (1995b), adopting the STMAG system zeropoints therein, and converting the resulting values to the BVI system using the iterative procedure described in Holtzman *et al.* (1995b), with coefficients from their Table 10. Figure 2 contains our final WFPC2 (I, $V-I$) color-magnitude diagram for IC 1613. Typical 1- σ errorbars at 24th magnitude are $\sigma_V = 0.03$, $\sigma_I = 0.04$. The distributions of magnitude vs. error are shown in Figure 3.

Along with magnitudes and standard errors, DoPHOT returns for each object a “quality” parameter, which allows the astronomer to discriminate true point sources from unresolved blends, background galaxies, and stars contaminated by cosmetic CCD blemishes. Because of the steep main-sequence luminosity function, the blending criterion most strictly winnows the photometric sample at faint magnitudes.

For this paper, we have retained in our analysis only those stars with the highest quality photometry (“Type 1”). The remainder of this paper considers only the 9,810 stars with superior F555W and F814W photometry, and the 1,639 stars with superior F439W photometry. Because of the small numbers of luminous, blue stars in our chosen field, the F439W photometry has been used solely to check our adopted reddening values for internal consistency.

The smoothly rising error curves in Figure 3 indicate that color-magnitude diagrams will not be systematically distorted by the effects of crowding (Dohm-Palmer *et al.* 1997a, Han *et al.* 1997). From experience with WFPC2 photometry, we estimate our 90% and 50% completeness levels in (V,I) fall at (23.8, 23.8), and (25.6, 25.2), respectively. Completeness issues are most problematic for the lower main-sequence and for the giant branch below the level of the red clump. Completeness is high over most of the magnitude range in Figures 2 and 3, decreasing smoothly towards fainter magnitudes; because most of our analysis deals with stars brighter than 24th magnitude, incompleteness is not expected to dramatically affect our results.

3.3. Observations with WIYN

To broaden our areal coverage of IC 1613, we obtained V and I images centered on the WFPC2 position with the 3.5-meter WIYN telescope at Kitt Peak, on 1–3 October, 1997. The best data, comprising 2×600 seconds in I and 900 seconds in V, were taken under photometric conditions with 0''.6 seeing. Additional exposures with $\sim 1''$ seeing totalling 1500 sec

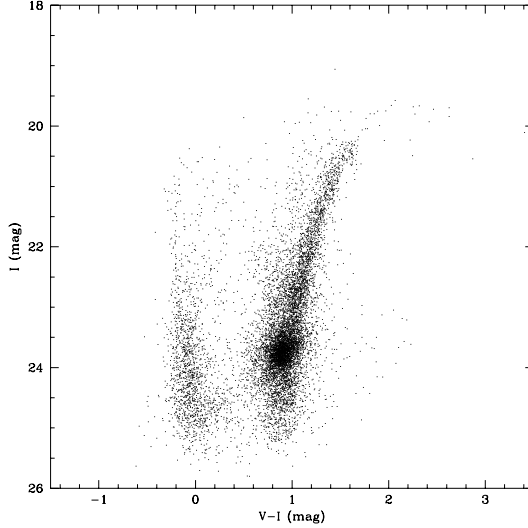


FIG. 2.— WFPC2 I, V–I color-magnitude diagram, including only stars for which DoPHOT achieved the best possible photometry. 9800 stars are shown. The most striking features of this CMD are the prominent red giant branch and the upper main-sequence.

Figure 3
can be obtained from
the following URL:

<http://www.astro.wisc.edu/~cole/ic1613.fig3.eps>

FIG. 3.— The distributions of magnitude vs. photometric error for our WFPC2 BVI photometry. The mean errors at 24th magnitude are $\sigma_V = 0.03$, $\sigma_I = 0.04$, $\sigma_B = 0.03$.

in each filter were obtained. The broad (6.8 square— ≈ 9 times the area of the WFPC2 field) field of view and fine image quality of the WIYN imager allow us to extend our CMD analysis to luminous, short-lived phases of stellar evolution which are typically under-represented in the WFPC2 field. A WIYN image of IC 1613, with the WFPC2 field overlaid for comparison, is shown in Figure 4.

The WIYN images were overscan corrected, bias-subtracted, and flat-fielded within IRAF’s `ccdproc` routines². We performed photometry using DoPHOT, as per the WFPC2 images, obtaining “Type 1” photometry for 14,678 VI pairs. We also observed standard fields from Landolt (1992) to reduce the data to a standard system for comparison to the WFPC2 data. The WIYN color-magnitude diagram is shown in Figure 5. Comparison to Fig. 2 shows good agreement regarding the magnitude of the tip of the red giant branch and the colors of the red giant branch and main-sequence. Comparison of individual stars on the red giant branch finds $I_{\text{WIYN}} = I_{\text{WFPC2}} - 0.04 \pm 0.03$, $(V-I)_{\text{WIYN}} = (V-I)_{\text{WFPC2}} + 0.04 \pm 0.04$.

4. COLOR-MAGNITUDE DIAGRAMS

Figures 2 and 5 show two main branches, and several smaller features, each of which contains stars with a range of ages and metallicites:

1. The red giant branch (RGB), between $V-I = 0.7-1.7$ and extending upwards to $I = 20.3$; the strongest feature of the CMD, contains stars from 500 Myr to $\gtrsim 10$ Gyr among its various substructures. The location of the RGB tip agrees well with the adopted distance to IC 1613.
2. The blue plume, blueward of $V-I = 0.2$, consisting primarily of main-sequence stars younger than ≈ 1 Gyr. The majority of blue plume stars in Figure 2 are expected to be of spectral class B; Figure 5 includes some probable O stars, indicators of very recent ($\lesssim 10$ Myr) star formation.
3. The red clump (RC), centered at $I = 23.76$, $V-I = 0.9$. This feature contains core-helium burning stars with ages between $\approx 1-10$ Gyr, and accounts for a plurality of the stars in Figure 2.
4. The blue loop (BL) stars, extending vertically from the RC to $I \approx 22.5$ before turning diagonally blueward to become indistinguishable from the main sequence at $I \approx 21$. These are the

younger counterparts to the RC stars. Crowding in Figure 5 renders them indistinguishable from the RGB.

5. The asymptotic giant branch (AGB), extending redward from the tip of the RGB, is weakly present in Figure 2, but more strongly apparent in the WIYN CMD. AGB stars indicate an intermediate-age population (2–6 Gyr). A horizontal AGB indicates metallicities of $\sim 1/10$ solar; additionally, a more metal-poor component lies along an upward extension of the RGB in Figure 5.
6. The red supergiants (RSG), extending nearly vertically to $I = 16.5$ at $V-I \approx 1.3$ in Figure 5. Fewer than 16 of these are expected to be foreground dwarfs (Bahcall & Soneira 1980); their possible presence does not compromise the reality of the IC 1613 RSG sequence. These young stars are on their way to an ‘onion-skin’ nuclear burning structure and are younger than a few 10^7 years. Such young stars should be representative of the most metal-rich population in IC 1613.
7. The horizontal branch, visible at the base of the RC as a blueward extension at $I = 24.3$, and possibly as a red extension from the main-sequence at $I = 24.7$. These are the most metal-poor, oldest (10–15 Gyr) core-helium burning stars in IC 1613, tracers of a population whose main-sequence turnoff would be expected to lie at $I \approx 28$. The gap in the horizontal branch between $0.3 \leq V-I \leq 0.6$ is consistent with the location of the RR Lyrae instability strip in the CMD.

The WFPC2 and WIYN color-magnitude diagrams contain stars as young as the dynamical timescale for protostellar collapse and potentially as old as the Galactic globular clusters. The salient features of the CMDs are summarized in Figure 6. The dividing point between the blue and red helium burners (HeB) has been defined here to be the Cepheid instability strip, by analogy to the blue and red horizontal branches. Each feature is marked according to the approximate logarithmic age expected for the given evolutionary phase; the prominence of the marker symbols provides a rough guide to the strength of the components of the CMD. Taken together, the CMDs provide an overall picture of the star-formation history of IC 1613: it appears to have formed stars over wide ranges of age, perhaps continuously; most of the

²IRAF is distributed by the National Optical Astronomy Observatories, which are operated by the Association of Universities for Research in Astronomy, Inc., under cooperative agreement with the National Science Foundation.

Figure 4
can be obtained from
the following URL:

<http://www.astro.wisc.edu/~cole/ic1613.fig4.eps>

FIG. 4.— 900-second, V band, WIYN image of the main body of IC 1613. North is up, East is to the left, and the WFPC2 field of view is overlaid. The seeing is $0''.6$, causing the background galaxies to stand out clearly through the stars of IC 1613.

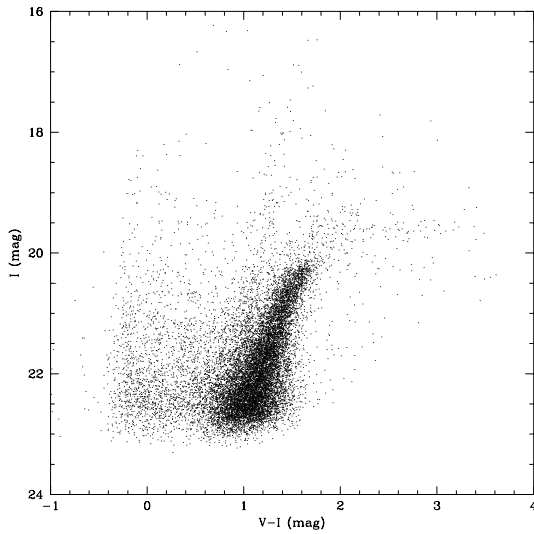


FIG. 5.— WIYN I, V-I color-magnitude diagram, including only stars for which DoPHOT achieved the best possible photometry. 14678 stars are shown. Image crowding has blended the red giant branch with blue loop stars and red supergiants, causing an artificially large color spread. The luminous red supergiants and extremely red tail of the asymptotic giant branch are more fully sampled by the $6''.8 \times 6''.8$ field of view.

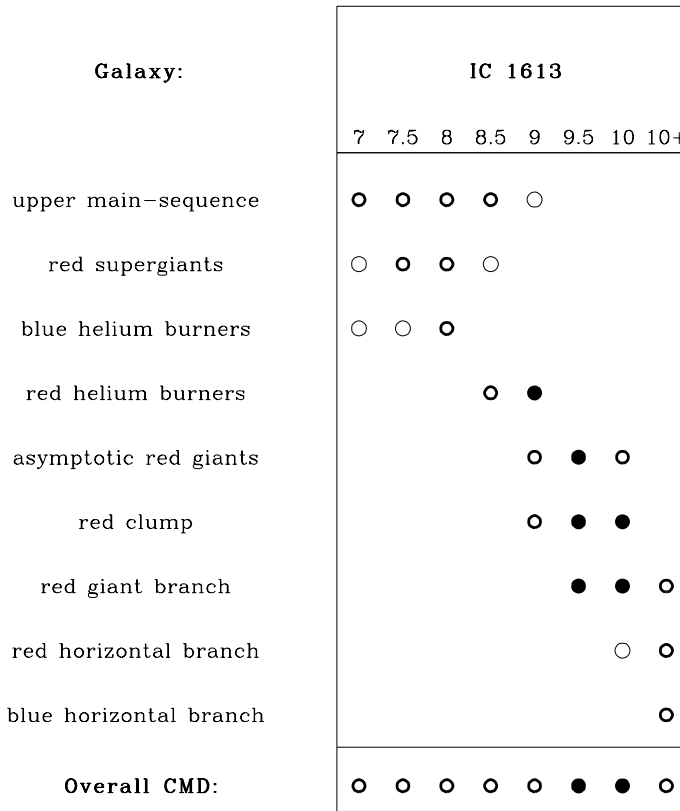


FIG. 6.— Reference card for the stellar populations at the center of IC 1613 as derived from the morphology of WFPC2 and WIYN color-magnitude diagrams. CMD features are associated with populations of various ages. The relative strength of each population is given by the shaded circles in the appropriate logarithmic age bins. A general picture of approximately continuous star formation emerges, although our ability to resolve “bursty” behavior becomes progressively poorer with age.

star-formation may have taken place a few to ten billion years ago. In subsequent sections of this paper, we examine the implications of CMD morphology for the star-formation history of IC 1613 in more detail.

We take the distance to IC 1613, from Lee *et al.* (1993), to be 715 kpc, corresponding to a distance modulus $(m-M)_0 = 24.27$. We correct for a small amount of interstellar reddening, $E_{B-V} = 0.03$ (Mateo 1998). We derive a value $E_{B-V} = 0.02 \pm 0.02$ from a comparison of the B–V and V–I colors of the upper main-sequence between $24 \geq V \geq 23$, using the intrinsic color of the zero age main-sequence as a template. We adopt the Galactic reddening law of Cardelli, Clayton & Mathis (1989), using $R_V = 3.1$, to derive extinction parameters $A_V = 0.093$, $A_I = 0.045$, and $E_{V-I} = 0.048$.

5. THE STELLAR POPULATIONS OF IC 1613

The mean color of the red giant branch, in a simple stellar population, can be used to estimate the metallicity of its stars. Da Costa & Armandroff (1990) give a calibration for globular clusters' metallicities using the mean, dereddened V–I color of their giant branches at an absolute magnitude $M_I = -3$. At the distance and reddening of IC 1613, this translates to $I = 21.25$. From the WFPC2 CMD, we use 47 stars to determine $V - I_0 = 1.29 \pm 0.07$; the much larger sample of 255 stars in the WIYN field yields $V - I_0 = 1.28 \pm 0.10$. The Da Costa & Armandroff (1990) calibration gives $[Fe/H]_{WFPC2} = -1.38 \pm 0.31$, and $[Fe/H]_{WIYN} = -1.43 \pm 0.45$. These abundance spreads are not solely due to photometric errors, which limit the resolution in $[Fe/H]$ to 0.17 dex for WIYN, and 0.13 dex for WFPC2; an intrinsic spread in color is present due to ranges in age and/or metallicity. Our estimate of $[Fe/H] \approx -1.4$ is in excellent agreement with the previous assessment $[Fe/H]_{RGB} = -1.3 \pm 0.8$ (Freedman 1988a). Although IC 1613 is certainly *not* a simple, single age stellar population, this calculation still provides a useful first estimate of the stellar metallicities (e.g., Da Costa 1998).

A real abundance variation is almost certainly present in IC 1613. However, the presence of intermediate-age (5–10 Gyr) stars, strongly suggested by the prominent red clump at $I \approx 23.8$, complicates the estimation of metallicity from RGB color. In stellar populations that are significantly younger than the globular clusters, the giant branches lie to the blue of the Da Costa & Armandroff (1990) calibration sequence, causing the $V - I_0$ method to underestimate the metallicity by up to ≈ 0.3 dex (see, e.g., Da Costa 1998). This is the infamous age-

metallicity degeneracy; the inferred metallicity range among IC 1613's red giants may be, in part, due to an age range. If age and metallicity are correlated (e.g., with chemical enrichment occurring over time), than it is possible to underestimate the range of metallicities among giant branch stars. Independent abundance information, together with detailed modelling of the star-formation history, is needed in order to lift the age-metallicity degeneracy.

To test our photometry, we rederived the distance to IC 1613 using the tip of the RGB in our WFPC2 CMD. We followed the metallicity calibration given by Lee *et al.* (1993), and applied a Sobel filter (Sakai, Madore & Freedman 1996) to the I-band luminosity function. This fixed the tip of the RGB at $I = 20.28 \pm 0.09$, which yields a distance modulus $(m-M)_0 = 24.29 \pm 0.12$ for $E_{B-V} = 0.03 \pm 0.02$ and $[Fe/H] = -1.38 \pm 0.31$. This is in excellent agreement with the adopted value of $(m-M)_0 = 24.27 \pm 0.10$.

5.1. Recent Star-Formation History

The young stellar populations of IC 1613 have been studied by Sandage & Katem (1976), Hodge (1978), Freedman (1988a,b), Hodge *et al.* (1991), and Georgiev *et al.* (1999). The picture that emerges from these studies is of a galaxy in which the central regions have undergone continuous star formation over the past 1–300 Myr, with the youngest stars clustered into small associations and possible clusters (Hodge 1978). While the regions of recent star formation are more centrally concentrated than the underlying old population, the very youngest stars seem to avoid the dead center of IC 1613 (Hodge *et al.* 1991). This partially accounts for the lack of blue stars brighter than $M_I \approx -3.5$ in the WFPC2 field of view.

Freedman (1988a) found that the main-sequence luminosity function brighter than $M_V = 21$ could be fit with a simple power law, similar to other Local Group dwarf irregulars, with $N(m) \propto m_V^{0.58 \pm 0.07}$. Freedman attributes a flattening of the luminosity function slope at $V \approx 21$ to crowding in her data. The WFPC2 V-band luminosity function is plotted in Figure 7. We find $N(m) \propto m_V^{0.48 \pm 0.09}$, marginally consistent with the steeper slope from Freedman (1988a)³. Statistical noise begins to dominate the WFPC2 main-sequence luminosity function brighter than $V \approx 21.5$; incompleteness due to crowding becomes problematic below $V \approx 24.5$. Within these limits, which roughly bracket the range of the B stars ($3\text{--}20 M_\odot$; ages between 10–350 Myr), the constant slope of the logarithmic luminosity function suggests an approximately constant star-formation rate. We integrate a Salpeter

³The luminosity function of IC 1613 is thus nearly identical to that of the Sextans A dwarf irregular, for which Dohm-Palmer *et al.* (1997a) found $N(m) \propto m_V^{0.44}$.

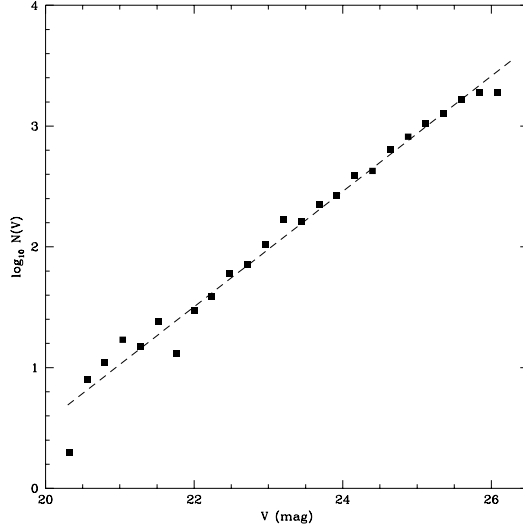


FIG. 7.— Main-sequence V-band WFPC2 luminosity function for all photometry. Incompleteness becomes a serious problem at $V \approx 24.5$. The least-squares fit slope is -0.48 ± 0.09 ; this includes stars as old as ≈ 350 Myr. Normalized for a Salpeter IMF this implies a mean SFR over that time of $3.5 \times 10^{-4} M_{\odot} \text{ yr}^{-1}$ across the 0.22 kpc^2 WFPC field of view.

IMF from 0.1 – $120 M_{\odot}$ to normalize the upper main-sequence luminosity function, and find a total star-formation rate of $3.5 \times 10^{-4} M_{\odot} \text{ yr}^{-1}$ across the WFPC2 field. At the distance of IC 1613, this corresponds to $1.6 \times 10^{-3} M_{\odot} \text{ yr}^{-1} \text{ kpc}^{-2}$.

For comparison, this is slightly smaller than the current star-formation rate in the brightest H II region (S10, a.k.a. complex 67), although S10 fills just one-tenth the area of the WFPC2 field and therefore sustains a much higher *intensity* of star-formation. This behavior is common to dwarf irregular galaxies; for example, Dohm-Palmer *et al.* (1997b) found that star formation in Sextans A has occurred in localized regions $\approx 10^2$ – 10^3 parsecs in size, and that these regions last for 100–200 Myr at a time.

Davidson & Kinman (1982) and Kingsburgh & Barlow (1995) have studied the Wolf-Rayet star DR 1 and its surrounding H II region; this object, presumably a few million years old, has an abundance between $Z \approx 0.004$ ($[\text{Fe}/\text{H}] = -0.7$, Kingsburgh & Barlow 1995) and $[\text{O}/\text{H}] = -1$ (Davidson & Kinman 1982). These are in reasonable agreement with the H II region nebular abundances reported by Skillman, Kennicutt, & Hodge (1989) of $[\text{O}/\text{H}] \approx -1.0$. Recent B star spectra (Kudritzki 1999) provide further support for the case that IC 1613 is currently forming stars with nearly the same metallicity as the Small Magellanic Cloud (Hodge 1989). The region of our present study was chosen to avoid known H II regions, and it is of interest to determine the highest metallicity attained during recent (but not current) star formation.

We can estimate the metallicity of the youngest stellar population in the WFPC2 field of view from the color extent of the blue loop stars—massive, core-helium burning stars—and the slope of the red supergiant sequence in the color-magnitude diagram. The WIYN CMD shows a well-populated RSG sequence, rising to $I \approx 16.5$; the spread in color of this sequence can be due to age as well as metallicity. From a comparison to theoretical isochrones (Girardi *et al.* 1999), the majority of the RSGs cannot be as metal-rich as $Z = 0.004$ ($[\text{Fe}/\text{H}] \approx -0.7$); the $Z = 0.001$ ($[\text{Fe}/\text{H}] \approx -1.3$) isochrones provide a better fit to the data.

While the RSG sequence above $I \approx 20$ is underpopulated in the WFPC2 CMD, the blue loop stars are prominent. We used a Monte Carlo code to compare the isochrones of Girardi *et al.* (1999) to this portion of the IC 1613 Hess diagram.⁴ Figure 8 shows the results of this simulation. We have sampled from the isochrone set assuming a constant star formation rate and Salpeter (1955) initial mass function for two metallicities, $Z = 0.001$ (left panel), and $Z = 0.004$ (right panel). In each panel of Figure 8 the star-formation rate was constant from 0.25–1 Gyr. The Hess diagram of the WFPC2 data is overplotted against the simulations, with isopleths from 2 – 256 decmag^{-2} ; each successive isopleth shows twice the CMD density of the previous one.

Figure 8 affords two main points of comparison between models and data. Firstly, the red HeB (blue loop) stars between $I \approx 23.5$ and 22 , with $V-I \lesssim$

⁴a contour plot of the number of stars per unit magnitude per unit color in the CMD—see Hess (1924); Trumpler & Weaver (1953)

Figure 8
can be obtained from
the following URL:

<http://www.astro.wisc.edu/~cole/ic1613.fig8.eps>

FIG. 8.— Synthetic CMDs created assuming a Salpeter IMF and constant star formation rate from 250–1000 Myr. The Hess diagram for IC 1613 is overlain. Left panel: model $Z = 0.001$. Right panel: model $Z = 0.004$. The red giant branch, older than 1000 Myr, has not been modelled here so that the locus of young giants and supergiants can be seen more clearly.

1; secondly, the base of the RSG plume with $I \lesssim 22$ and $V-I \approx 1$. Dohm-Palmer *et al.* (1997b) presented the first unambiguous detection of the blue loop stars in a metal-poor system and showed how these stars can be used to infer the star formation history of a galaxy over the past 1 Gyr. The clearest inference from Fig. 8 flows from the termination of the blue loop sequence at $I \approx 22$; this morphology indicates a higher past star-formation rate that declined at some point; the age of decline is metallicity dependent: 300 Myr for $Z = 0.004$, 400 Myr for $Z = 0.001$. The extent of the blue loop sequence in the models is clearly metallicity dependent; we see from Fig. 8 that the $Z = 0.001$ models are bluer than the data, while the $Z = 0.004$ models are too red. The same behavior can be seen with respect to the RSG sequence. An intermediate metallicity, $Z \approx 0.002$, is therefore predicted for the 0.1 – 1 Gyr old stellar populations of IC 1613. This value is in excellent agreement with the nebular abundances of Skillman *et al.* (1989) and Davidson & Kinman (1982).

We have not directly compared the IC 1613 Hess diagram to the WIYN CMD; these data do not reach beyond 100 Myr on the main-sequence, and are thus unmodelled by the Girardi *et al.* (1999) isochrone set. As in the WFPC2 CMD, the $Z = 0.004$ models are too red when compared to the RSG plume. Even the $Z = 0.001$ model blue loops do not reach far to the blue as the blue loops in the WIYN CMD above $I \approx 21.5$. If the models, and the photometry, can be trusted on this point, this would be indicative of a metallicity well below $Z = 0.001$ for the youngest generation of stars in IC 1613. However, comparison of the WIYN

and WFPC2 CMDs shows that crowding errors affect even the brighter stars in ground-based images (see, e.g., Tolstoy *et al.* 1998). Additionally, it has been shown that the color extent of blue loops in models of massive stars is quite sensitive to the adopted input physics (e.g., Chiosi 1998; Langer 1998); effects such as the mass-loss prescription, semiconvection, and rotation (e.g., Langer & Maeder 1995) can lead to a wide variety of blue loop morphologies at a given age and metallicity.

5.2. Intermediate-Age and Old Stellar Populations

Baade (1963) and Sandage (1971a) noted the elliptical sheet of red stars within which the main body of IC 1613 is embedded; drawing on Baade's (1944) division of the stellar populations of the more luminous Local Group galaxies into Populations I and II, this sheet has been identified with the Pop II element of IC 1613. Freedman's (1988a) photometry resolved this sheet into red giant and asymptotic giant branches, to a level of $V \approx 23$, confirming the presence of stellar populations aged at least ≈ 1 Gyr, and perhaps as old as the most ancient Galactic stars, 10–15 Gyr old.

Our WIYN color-magnitude diagram extends Freedman's (1988a) results; the strongest feature of the WIYN CMD (Fig. 5) is the classic Pop II red giant branch. We detect red giants to a limiting magnitude of $I \approx 23$ ($V \approx 24$) across the whole of the 6.8×6.8 field of view. Although the center of IC 1613 has not seen significant recent star formation and is the site of a hole in the H I distribution (Lake & Skillman 1989), the stars of our WIYN image (Fig. 4) show no tendency to avoid this area. This is in agreement

with the results of Hodge *et al.* (1991), who noted the differing behaviors of the bright blue stars and the faint red stars in this regard.

Because of the near-degeneracy of the red giant branch $V-I$ color to age beyond 2 Gyr, it has not previously been possible to infer the age mixture of the Baade's sheet population in IC 1613 from CMD morphology (Freedman 1988a); to resolve this issue requires photometry further down the main-sequence. Saha *et al.* (1992) identified 15 RR Lyrae-type variable stars in IC 1613; these betray the presence of a genuinely ancient stellar population in this galaxy. The observed variation in RR Lyrae production efficiency among Galactic globular clusters is evidence of an unknown (“second”) parameter which impacts the horizontal branch morphology of ancient stellar populations (van den Bergh 1967; Lee *et al.* 1994). This effect limits the power RR Lyrae number counts to constrain the precise contribution of ancient stars to the IC 1613 RGB; a lower limit of 15% was placed on the fraction of red giants older than ≈ 10 Gyr.

5.2.1. The Horizontal Branch

The presence of a red horizontal branch (RHB) population in the WFPC2 VI color-magnitude diagram can be discerned, in the color range $V-I \approx 0.6-0.8$, at $I \approx 24.2-24.3$. This is consistent with the mean g magnitude (Thuan & Gunn 1976) of 24.9 found by Saha *et al.* (1992) for the IC 1613 RR Lyraes. The Pop II stars of the central 500 pc of IC 1613 thus seem similar to the those in the relatively distant field studied by Saha *et al.* (1992). The theoretical RHBs of recent isochrone sets (e.g., Girardi *et al.* 1999) predict a magnitude of $I \approx 24.35$, for a metal abundance of 1/19 solar ($Z = 0.001$, corresponding to $[\text{Fe}/\text{H}] = -1.3$) at the distance of IC 1613. The -0.15 mag offset between the observed RHB and model isochrones can be accounted for by a difference in $[\text{Fe}/\text{H}]$ of ≈ -0.5 to -0.7 dex (Caloi, D’Antona & Mazzitelli 1997), suggesting a metallicity for the RHB population of $[\text{Fe}/\text{H}] \approx -1.8$ to -2.0 .

The red spur which extends from the main-sequence to $V-I \approx 0.3$ at $I \approx 24.7-24.8$ cannot be definitively assigned to a specific evolutionary state without further analysis. At least two different classes of stellar population can create such a feature in the color-magnitude diagram. The red spur could be post-main-sequence-turnoff stars aged 900 to 1100 million years with $Z = 0.001$; alternatively, its color and magnitude are consistent with the blue horizontal branch (BHB) of a 10–15 billion year old population of very low metallicity ($Z \approx 0.0004$).

The BHB interpretation shows consistency with previously known properties of IC 1613: its old average age, the inferred metallicity of the red horizontal

branch stars, and the detection of RR Lyrae variables by Saha *et al.* (1992). It is nigh impossible to precisely predict the expected number of BHB stars from IC 1613’s RGB luminosity function, because the RGB is likely contaminated with intermediate-age stars, and because the second parameter effect decouples horizontal branch morphology from the known physical properties of ancient stellar populations. Nevertheless, we performed a simple analysis to estimate the relative star-formation rates required to fully populate the red spur with BHB stars. We used a Monte Carlo technique to draw stellar populations from the Girardi *et al.* (1999) isochrones according to the initial mass function of Salpeter (1955) from $0.7-5 M_{\odot}$, to reproduce the relative numbers of stars seen in the red spur and on the main-sequence at the same I magnitude. From this we infer that the star-formation rate 15 Gyr ago was some 2–200 times larger than the recent ($t \lesssim 0.9$ Gyr) star-formation rate. The limiting uncertainty in this calculation is the second parameter effect (see Saha *et al.* 1992). The main-sequence turnoff associated with this dominant, ancient population would be located at $I \approx 27.5-28$, requiring an 8-meter class telescope to photometer reliably.

We used the same analysis technique to evaluate the hypothesis that the red spur at $I \approx 24.7$ is the subgiant branch produced by a burst of star formation ≈ 1 billion years ago. We divided the stars in this region of the CMD ($25 > I > 24.3$) into two color bins: a “main-sequence” bin from $-0.4 < V-I < 0.1$, and a “red spur” bin from $0.1 < V-I < 0.5$. The number ratio of main-sequence stars to spur stars is 2.08, which can be reproduced with models in which the star-formation rate from 900 to 1100 million years ago was a factor of 30 higher than before or since.

This large increase in star-formation rate would have dramatic consequences for the color-magnitude diagram of IC 1613, as well as for the galaxy itself. A sharp discontinuity in the WFPC2 main-sequence luminosity function would be present at $I \approx 25.1$, corresponding to the main-sequence turnoff of the putative 1 Gyr burst. Past experience with WFPC2 photometry (e.g., Dohm-Palmer *et al.* 1997a, Gallagher *et al.* 1998) suggests that our photometry is $\approx 50\%$ complete at this level. Using all of the WFPC2 photometry, we find rising power-law luminosity function down to $I \approx 26$ with a sharp decline due to incompleteness below that level.

Although increasing photometric errors prevent the lower main-sequence luminosity function from *absolutely* ruling out a factor of 30 increase in star-formation rate a billion years ago, the stars of the red clump and giant branch are not compromised by these problems. A large 1 billion year-old population will produce a very distinctive “vertical red clump”,

or pseudo-clump, concentrated in color between $0.7 \lesssim V-I \lesssim 0.9$ and stretching from $M_I \approx 0$ to -1.2 (Caputo, Castellani & Degl'Innocenti 1995; Girardi *et al.* 1998). The model which best reproduces the ratio of stars in the red spur to stars on the main-sequence predicts a ratio of pseudo-clump stars to brighter RGB stars of 6.8, which is inconsistent with our observed ratio of 1.5. While IC 1613 shows a pseudo-clump, its extension to $I \approx 22$ ($M_I \approx -2.25$) suggests a period of more or less continuous star formation from 400–1200 Myr ago.

A further inconsistency with the 1 Gyr burst scenario for the red spur is the relative lack of stars between $V-I \approx 0.3$ and 0.6; subgiant stars evolve quickly through this region of the CMD, but at a smoothly increasing rate. The red edge of the spur at $V-I \approx 0.3$ would imply a sudden acceleration in the pace of stellar evolution of low-mass stars which is not predicted by theoretical models (e.g., Girardi *et al.* 1999). Contrariwise, the color gap is consistent with the location of the RR Lyrae instability strip; such gaps are observed in the horizontal branches of many systems (e.g., the Carina dwarf spheroidal galaxy—Smecker-Hane *et al.* 1994).

5.2.2. The Asymptotic Giant Branch

The strong AGB seen in the WIYN CMD (61 stars redder than $V-I = 1.8$, with I from 19.2–20.0) is evidence of a large, intermediate-age stellar population in IC 1613. 17 of these stars are also present in the WFPC2 CMD. In the WIYN image, the density of AGB stars is highest along the bar of the galaxy, and decreases with increasing distance from the main body of the galaxy. The AGB density does not increase towards the areas of current star formation, northeast of the bar.

Cook, Aaronson & Norris (1986) developed a relation between C/M star ratios and heavy element abundances, which was used by Cook & Aaronson (1988) to find a metallicity of $[\text{Fe}/\text{H}] \leq -1.0$ for the intermediate-age stars in IC 1613. Our WIYN I-band AGB luminosity function resembles the C-star luminosity function of Cook *et al.* (1986) above $I \approx 20$, where their sample becomes incomplete. Scaling the 14 detected carbon stars from Cook *et al.* to the WIYN field of view predicts ≈ 87 carbon stars; because the very red stars are somewhat clustered towards the northwest quadrant of the WIYN image, where one of the Cook *et al.* fields was located, this overprediction is not a cause for concern. Conversely, it is not unreasonable to expect a large fraction of our 61 AGB stars to be bona fide carbon stars. Cook *et al.* (1986) found the carbon star fraction among extended AGB stars to be 75%–95% in their two fields.

Mould & Aaronson (1982) recognized the fact that

upper AGB stars are a tracer of 2–6 billion year old stellar populations, and used the luminosity extent of the AGB as an indicator of stellar age. Reid & Mould (1990) examined the AGB population of the Small Magellanic Cloud and found that, like IC 1613, the SMC has a high fraction of carbon stars among the faint ($-3 \leq M_{\text{bol}} \leq -5.5$) AGB stars. From the AGB luminosity function, Reid & Mould concluded that the mean age of the SMC is greater than 2–3 Gyr.

We perform a similar analysis, adopting the carbon star bolometric correction from Reid & Mould (1985), $BC_I = 1.9 - 0.7(V-I)_0$. The resulting luminosity function for our WIYN data is shown in Figure 9. The M_{bol} -age relation from Table 3 of Mould & Aaronson (1982) is marked with open stars and labelled according to age. Incompleteness is increasing towards *brighter* M_{bol} : the most luminous stars in Figure 9 are located at $V \approx 22.5$, near the limit of the WIYN data. Therefore we may be biased towards the detection of somewhat older carbon stars.

It is clear from Figure 9 that IC 1613 has formed substantial numbers of AGB stars over a long period of time. The lack of AGB stars younger than 2 Gyr is partially due to the decreasing stellar lifetimes with decreasing age. However, a higher star formation rate during ancient times than during recent ones is consistent with the presence of the blue horizontal branch stars. Information derived from such an advanced phase of stellar evolution is subject to compounded uncertainties (see, e.g., Chiosi 1998). Marigo, Girardi & Chiosi (1996), for example, had difficulty reproducing the distribution of carbon stars in SMC clusters with existing models; even with the latest models, Marigo & Girardi (1998) found that the shape of the carbon star luminosity function is relatively insensitive to the form of the star-formation history of a galaxy. Therefore we decline to draw quantitative conclusions regarding the variation of star-formation rate over the past 2–10 Gyr of IC 1613's history.

5.2.3. The Red Clump

The relative strengths of the ancient and middle-aged stellar populations in dwarf irregular galaxies are still very uncertain (e.g., Tolstoy 1998; Da Costa 1998; Mateo 1998). The strong red clump in Figure 2 is an indication of the number of 1–10 Gyr old stars. Because the red clump stars share a common core mass ($M_c \approx 0.5 M_{\odot}$), their helium-burning lifetimes do not increase rapidly with increasing age (decreasing total mass) from ages ≈ 1.2 –10 Gyr. In contrast, the RGB lifetime is a strongly decreasing function of stellar mass. The ratio of RC stars to RGB stars in a CMD can therefore be used as a rough estimate of the mean age of a stellar population (see, e.g., Han

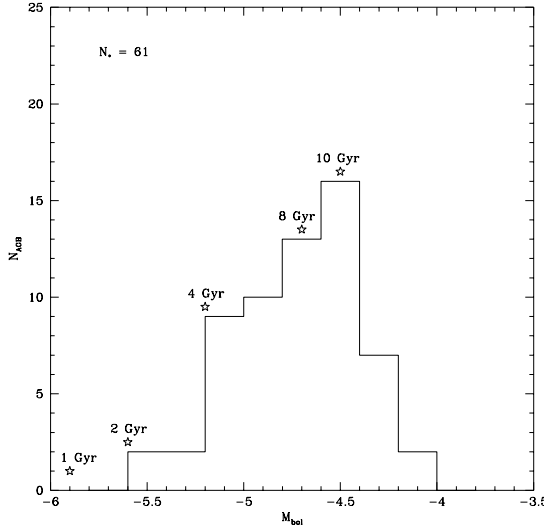


FIG. 9.— Bolometric luminosity function of AGB stars in the WIYN field. Results from the carbon star M_{bol} -age relation of Mould & Aaronson (1982) are marked with stars; star formation has been, on average, a continuous process throughout the lifetime of IC 1613, although relative star-formation rates cannot be accurately inferred from this figure due to model uncertainties and small number statistics.

et al. 1997, Gallagher *et al.* 1998, Tolstoy 1998).

In the WFPC2 CMD of IC 1613, the number ratio of RC to RGB stars is 2; because photometric completeness at the level of the red clump ($V, I \approx 24.6, 23.8$) is $\approx (80\%, 90\%)$, we take our value $N(\text{RC})/N(\text{RGB}) \geq 2$ to be a lower limit. Examination of synthetic CMDs therefore provides an upper limit to the mean age of the RGB-producing population: $t_{\text{RGB}} \leq 7 \pm 2$ Gyr. The ratio of RC to RGB lifetimes has a slight metallicity dependence, such that a more metal-rich population is older than a metal-poor one at a given $N(\text{RC})/N(\text{RGB})$ (Cole 1999, in preparation).

We can make a further estimate of the mean age of the red clump stars using its mean I magnitude. The magnitude of the red clump depends on its metallicity and, to a lesser extent, its age (e.g., Girardi *et al.* 1998; Seidel, Demarque, & Weinberg 1987). To define the magnitude of the red clump, we plot the WFPC2, I -band luminosity function in Figure 10. The mean magnitude of the red clump stars is $I = 23.76$, and the dispersion about the mean is $\sigma = 0.33$. This mean magnitude corresponds to an absolute magnitude $M_I = -0.56$.

If we adopt the mean RGB metallicity of $[\text{Fe}/\text{H}] = -1.4$ for the red clump, we can then solve for the mean age which produces a clump of the correct brightness for that metallicity. This is most conveniently done relative to the Solar neighborhood, where $M_I(\text{RC}) = -0.23 \pm 0.03$ (Stanek & Garnavich 1998). From Cole (1998), we find that the mean age of the IC 1613 red clump is approximately equal to that of the Solar neighborhood, $t \sim 6$ Gyr (e.g.,

Jimenez, Flynn, & Kotoneva 1998).

Both of these estimates are subject to strong systematic error. Contamination of the RC by stars in the 800–1200 Myr age range can bias the measured $M_I(\text{RC})$ either high or low, depending on the exact star formation and chemical enrichment histories. Photometric completeness decreases by a small amount across the magnitude range of the clump, and may induce a slight bias toward younger ages. On a more fundamental level, there is still some question as to whether the red clump magnitude varies with age between 2–10 Gyr as models predict—Udalski (1998) argues that the clump magnitude does not vary with age in a sample of Magellanic Cloud star clusters; however, Girardi (1999) finds that the predicted fading with age is not ruled out by Udalski’s data. Despite the formidable observational and theoretical uncertainties in the analysis, we feel that our main conclusion—that IC 1613 is dominated neither by 10–14 Gyr old stars nor by 1–4 Gyr old stars, but contains stars of all ages—is robust.

We can further use the red clump to constrain the metallicities of the stellar populations of IC 1613 at various ages. The “pseudo-clump”, which overlays the red clump but consists of stars just above the maximum mass of core-helium flash ($1.7\text{--}2.0 M_{\odot}$, e.g., Sweigart, Greggio & Renzini 1990) contains stars $\approx 1\text{--}1.2$ Gyr old. The color of this feature has a strong metallicity-dependence (Girardi *et al.* 1998); from the lower limit of $V-I \approx 0.75$ for the red clump we find a lower limit of $[\text{Fe}/\text{H}] \approx -1.5$ for the 1–1.2 Gyr population.

The fading of the red clump with increasing age and

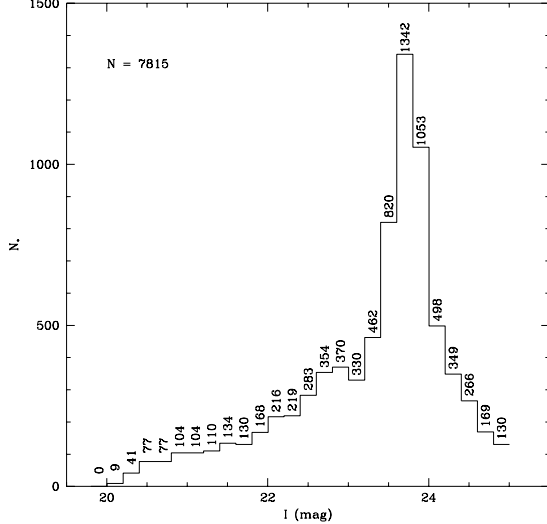


FIG. 10.— RGB I-band luminosity function, highlighting the red clump. The mean magnitude of the clump is $I = 23.76 \pm 0.30$. The red clump here contains a mixture of post-core-helium flash, “true” clump stars, older than 1.2 Gyr, and more massive stars aged 0.8–1.2 Gyr. This combination and growing incompleteness at the faint end complicate the interpretation of the clump.

metallicity allows us to put an upper limit on $[\text{Fe}/\text{H}]$ for the very old stars in IC 1613, using the magnitude of the horizontal branch and lower red clump. For ages older ≈ 6 Gyr, the $Z = 0.004$ ($[\text{Fe}/\text{H}] = -1.3$) isochrones from Girardi *et al.* (1999) become too faint to match the observed red clump in IC 1613. This is essentially the same effect that we have seen for the red horizontal branch stars, which have $[\text{Fe}/\text{H}] \approx -1.9$.

6. DISCUSSION

The analysis of stellar populations allows us to construct a rough age-metallicity relation for IC 1613. Previous determinations of IC 1613’s global metallicity have mainly been from nebular spectroscopy (e.g., Skillman *et al.* 1989). These measures sample only the youngest component of IC 1613, and have established the current metal abundance of IC 1613 at $[\text{Fe}/\text{H}] \approx -1$. Freedman (1988a) assessed the RGB abundance, sampling the stars from 2–14 Gyr old; Cook & Aaronson (1988) judged the upper limit of $[\text{Fe}/\text{H}]$ to be ≤ -1 for the 2–6 Gyr population, using the ratio of C to M stars along upper AGB.

In this paper, we have estimated the metal abundance of the blue and red supergiants to be $[\text{Fe}/\text{H}] \approx -1$, providing an abundance indicator for stars in the 10–500 Myr range. We reappraised the metallicity of the RGB, finding $[\text{Fe}/\text{H}] = -1.4 \pm 0.3$. Using the morphology of the red clump, we provide an upper limit of $[\text{Fe}/\text{H}] \lesssim -1.3$ for the stars older than ≈ 6 Gyr. And from the magnitude of the horizontal branch stars, we infer a metallicity for the oldest stars in IC 1613 of $[\text{Fe}/\text{H}] \sim -1.9$. We have assembled these data into Figure 11, our preliminary

age-metallicity relation for IC 1613. Overplotted is an age-metallicity relation for the Small Magellanic Cloud, from Pagel & Tautvaišienė (1998). Despite the large uncertainties, it appears that the chemical evolution of IC 1613 has taken a similar form to that of the SMC, although IC 1613 may be slightly more metal-poor. Figure 11 quantifies to an extent the “population box” diagram given in Hodge (1989), although we find a stronger trend of metallicity with age than the population box constructed from older data by Grebel (1998).

Where do IC 1613’s stellar populations place it within the context of the Local Group dwarf galaxies? Many Local Group dwarfs have now been studied with WFPC2 to a comparable depth as IC 1613, and so we can begin to use direct intercomparisons to test the accuracy of model-dependent interpretations of CMDs in terms of galaxy evolution. In Figure 12, we plot the grayscale Hess diagrams of four Local Group dwarf galaxies, and overplot the Hess diagram of IC 1613 for comparison. The basic parameters of each galaxy, taken from Mateo (1998), are given in Table 2. The quantities $\Delta(m-M)$ and ΔE_{B-V} denote the offsets applied to the data for each galaxy in order to compare the Hess diagrams to IC 1613. Each diagram is constructed from WFPC2 F555W and F814W data, and plotted with a logarithmic transfer function.

6.1. NGC 147

NGC 147 is a dwarf elliptical satellite of M31; the WFPC2 data are from Han *et al.* (1997). Its RGB extends further to the red than IC 1613’s, due to the

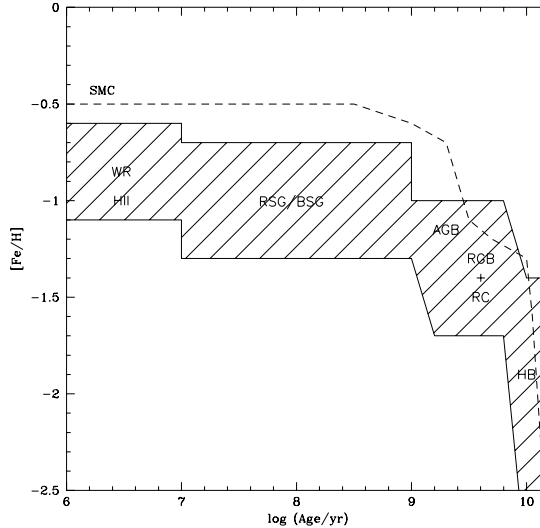


FIG. 11.— Age-metallicity relation for IC 1613. Each region of the figure is labelled with the CMD feature that constrains the metallicity to lie within the shaded region. Abbreviations are as given in the text; WR denotes the Wolf-Rayet star; HII denotes the H II regions. The dotted line shows the mean age-metallicity relation for the SMC.

TABLE 2
FOUR LOCAL GROUP DWARFS

Galaxy	$\Delta(m-M)$	ΔE_{B-V}	M_V	[Fe/H]	M_{HI}/L_B
IC 1613	-15.2	-1.4	0.81
NGC 147 ^a	0.05	0.15	-15.5	-1.1	<0.001
Pegasus ^b	0.5	0.12	-12.9	-1.3	0.44
Leo A ^c	0.0	0.0	-11.4	-1.7	1.6

^aHan *et al.* 1997.

^bGallagher *et al.* 1998.

^cTolstoy *et al.* 1998.

Figure 12
can be obtained from
the following URL:

<http://www.astro.wisc.edu/~cole/ic1613.fig12.eps>

FIG. 12.— Greyscale Hess diagrams for 4 Local Group dwarf galaxies of similar luminosity: IC 1613, NGC 147, Pegasus, and Leo A. The IC 1613 logarithmic Hess diagram is contoured atop each panel to highlight the similarities and differences between them.

higher mean abundance (and/or age) of NGC 147. Concordantly, the NGC 147 red clump lies ≈ 0.1 mag below IC 1613's. The upper main-sequence is unpopulated in NGC 147, a sign that star-formation ended at least ≈ 1 Gyr ago (Han *et al.* 1997). A blue horizontal branch population is prominent in NGC 147, sharing its locus in the Hess diagram with that of IC 1613. In NGC 147, star-formation went nearly to completion early in its history, enriching subsequent generations of stars, which now populate the RGB.

6.2. *Pegasus*

As mentioned above, Pegasus is a transition galaxy between the dwarf irregular and dwarf spheroidal classes; it is also one of IC 1613's nearest neighbors within the Local Group. Though less massive and less luminous than IC 1613, Pegasus is of comparable metal abundance to IC 1613, and has a similar RGB and main-sequence morphology. However, Pegasus has a larger AGB population than IC 1613, as would be expected from its enhanced period of star-formation a few Gyr ago (Gallagher *et al.* 1998). The recent star-formation rate in the WFPC2 field, $\dot{M} \approx 1600 \text{ M}_\odot \text{ Myr}^{-1} \text{ kpc}^{-2}$, is similar to that derived by Gallagher *et al.* (1998) for Pegasus, $\dot{M} = 1350-2000 \text{ M}_\odot \text{ Myr}^{-1} \text{ kpc}^{-2}$; however the WFPC2 image of IC 1613 excludes the most active regions of star formation. Pegasus and IC 1613 may be examples of galaxies which undergo occasional strong episodes of star-formation lasting up 0.5–1 Gyr, at intervals of one to a few Gyr. The differences in their recent (< 3 Gyr) star-formation histories would then be due to a difference in phase in their cycles of quiescent vs. elevated star-formation.

6.3. *Leo A*

Leo A provides a stark contrast to the other galaxies in this sample. The color-magnitude data are from Tolstoy *et al.* (1998). The smallest, most isolated galaxy in the sample, the CMD of Leo A shows the unusual feature of a dominant blue supergiant branch, evidence for strong recent star formation. Leo A's giant branch lies to the blue of IC 1613's, indicating its lower metallicity (and/or age). The blue, vertically extended red clump in Leo A suggests that this galaxy is dominated by an ≈ 1 Gyr population. Deep WIYN & MMT images of Leo A have failed to reveal an extended Baade's sheet population of red giants that would be indicative of significant early star formation (A. Saha, private communication, Tolstoy *et al.* 1998). The low metallicity and high gas fraction of Leo A are all consistent with a galaxy that has not had a major star formation episode until quite recently. Leo A is even more isolated than IC 1613 (its nearest neighbors are the Leo I and Leo II dwarf

spheroidals, more than 450 kpc away), and it must stand as a counterexample to the Tucana dwarf, a purely old system (Da Costa 1998), in evolutionary studies of small, isolated galaxies.

7. SUMMARY

We have used WFPC2 to obtain deep images of the dwarf irregular galaxy IC 1613. We analyze the resulting (I, V–I) color-magnitude diagrams to study the stellar populations at the center of this object. The strongest feature of the CMD is the red giant branch and superposed red clump. We find a mean metallicity of $[\text{Fe}/\text{H}] = -1.4 \pm 0.3$ from the color of the RGB, consistent but slightly lower than previous results (Freedman 1988). Upper main-sequence stars are also present, indicating a continuous period of star-formation during the past ≈ 350 Myr at a level of $\sim 3.5 \times 10^{-4} \text{ M}_\odot \text{ yr}^{-1}$ per WFPC2 field, corresponding to $1600 \text{ M}_\odot \text{ Myr}^{-1} \text{ kpc}^{-2}$. From a comparison of the supergiant stars to theoretical stellar evolution models, the mean chemical abundance during the past 800 Myr has been approximately one-tenth solar, consistent with previous measurements of H II region abundances.

In our WIYN image, we find 61 candidate carbon stars which populate an extended upper asymptotic giant branch and trace intermediate-age (2–10 Gyr) stellar populations. The AGB luminosity function indicates broadly continuous star formation from at least 4–10 Gyr ago; a possible decline since then can be neither confirmed nor ruled out with the present data.

We have detected for the first time a blue horizontal branch population in IC 1613. This very old population is not indicative of the IC 1613 RGB in general: from an analysis of the red clump stars, we find a mean age for the RGB of $t \lesssim 7 \pm 2$ Gyr. Systematic effects are unlikely to push this value upwards by the factor of ~ 2 necessary to enforce coevality with the blue horizontal branch.

We present a preliminary age-metallicity relation for IC 1613. While crude, this relation shows the same form as that of the Small Magellanic Cloud. We will use the age-metallicity information in a detailed modelling of the IC 1613 CMD in a subsequent paper. A comparison to WFPC2 CMD's of the galaxies Leo A, NGC 147, and Pegasus shows that the stellar populations of IC 1613 are very similar to those of Pegasus. Pegasus has an excess of bright AGB stars indicating elevated star formation a few Gyr in the past, while IC 1613 shows a higher level of current star formation; but both galaxies seem to have experienced a relatively constant, low level of star formation throughout their histories. Relatively isolated Local Group dwarf galaxies display a considerable

range in their star-formation histories, from objects where star formation was completed several Gyr in the past (e.g., Tucana—Lavery *et al.* 1996; possibly NGC 147—Han *et al.* 1997), to young-star dominated systems such as Leo A (Tolstoy *et al.* 1998).

This research was carried out by the WFPC2 Investigation Definition Team for JPL and was sponsored by NASA through contract NAS 7-1260. JSG and AAC acknowledge travel support from ESO for a visit to Garching bei München. We would also like to

thank Léo Girardi for making the latest isochrones of the Padua group available in advance of publication. It is a pleasure to thank the WIYN Telescope support staff for their excellent assistance at Kitt Peak. AAC thanks Dr. J.C. Howk for coffee and suggestions regarding the presentation of Hess diagrams. This research made use of the NASA Astrophysics Abstract Service, and the Canadian Astronomy Data Centre, which is operated by the Herzberg Institute of Astrophysics, National Research Council of Canada.

REFERENCES

Aparicio, A., Gallart, C., Bertelli, G. 1997, AJ, 114, 680.

Baade, W. 1928, Astronomische Nachrichten, 234, 407 (#5612).

Baade, W. 1935, Report of the Director of Mt. Wilson Observatory, 1934-35, p. 184.

Baade, W. 1944, ApJ, 100, 137.

Baade, W. 1963, "The Evolution of Stars and Galaxies", ed. C. Payne-Gaposchkin, (Cambridge: Harvard Univ. Pr.), p. 15.

Bahcall, J.N., & Soneira, R.M. 1980, ApJS, 44, 73.

Burstein, D., & Heiles, C. 1982, AJ, 87, 1165.

Caloi, V., D'Antona, F., & Mazzitelli, I. 1997, A&A, 320, 823.

Caputo, F., Castellani, V., & Degl'Innocenti, S. 1995, A&A, 309, 413.

Cardelli, J.A., Clayton, G.C., & Mathis, J.S. 1989, ApJ, 345, 245.

Chiosi, C. 1998, in "Stellar Astrophysics for the Local Group", edited by A. Aparicio, A. Herrero, & F. Sánchez, (Cambridge: Cambridge Univ. Pr.), p. 1.

Cole, A.A. 1998, ApJ, 500, L137.

Cook, K.H., & Aaronson, M. 1988, PASP, 100, 1218.

Cook, K.H., Aaronson, M., & Norris, J. 1986, ApJ, 305, 634.

Da Costa, G.S. 1998, in "Stellar Astrophysics for the Local Group", edited by A. Aparicio, A. Herrero, & F. Sánchez, (Cambridge: Cambridge Univ. Pr.), p. 351.

Da Costa, G.S., & Armandroff, T.E. 1990, AJ, 100, 162.

Davidson, K., & Kinman, T.D. 1982, PASP, 94, 634.

Dohm-Palmer, R.C., Skillman, E.D., Saha, A., Tolstoy, E., Mateo, M., Gallagher, J.S., Hoessel, J.G., Chiosi, C., & Dufour, R.J. 1997a, AJ, 114, 2514.

Dohm-Palmer, R.C., Skillman, E.D., Saha, A., Tolstoy, E., Mateo, M., Gallagher, J.S., Hoessel, J.G., Chiosi, C., & Dufour, R.J. 1997b, AJ, 114, 2527.

Ellis, R.S. 1997, ARA&A, 35, 389.

Freedman, W.L. 1988, AJ, 96, 1248.

Freedman, W.L. 1988, in ASP Conf. Ser. 4, eds. S. van den Bergh & C. Pritchett, (Provo: Brigham Young Univ. Pr.), p. 24.

Gallagher, J.S., Tolstoy, E., Dohm-Palmer, R.C., Skillman, E.D., Cole, A.A., Hoessel, J.G., Saha, A., & Mateo, M. 1998, AJ, 115, 1869.

Georgiev, I., Borissova, J., Rosado, M., Kurtev, R., Ivanov, G., & Koenigsberger, G. 1999, A&AS, 124, 21.

Girardi, L. 1999, MNRAS, submitted, astro-ph/9901319.

Girardi, L., Groenewegen, M.A.T., Weiss, A., & Salaris, M. 1998, MNRAS, 301, 149.

Girardi, L., Bressan, A., Bertelli, G., & Chiosi, C. 1999, MNRAS, in preparation.

Grebel, E.K. 1998, in "The Stellar Content of Local Group Galaxies" IAU Symp. 192, eds. P. Whitelock & R. Cannon, in press, astro-ph/9812443.

Grebel, E.K., & Guhathakurta, P. 1999, ApJ, 515, L101.

Han, M., Hoessel, J.G., Gallagher, J.S., Holtzman, J., Stetson, P.B., & the WFPC2 IDT 1997, AJ, 113, 1001.

Hess, R. 1924, "The Distribution Function of Absolute Brightness", in Seeliger Festschrift, ed. H. Kienle, (Berlin: Springer), p. 265.

Hodge, P.W. 1978, ApJS, 37, 145.

Hodge, P.W. 1989, ARA&A, 27, 139.

Hodge, P.W., Lee, M.G., & Gurwell, M. 1990, PASP, 102, 1245.

Hodge, P.W., Smith, T.R., Eskridge, P.B., MacGillivray, H.T., & Beard, S.M. 1991, ApJ, 369, 372.

Holtzman, J.A., Hester, J.J., Casertano, S., Trauger, J.T., Watson, A.M., & the WFPC2 IDT 1995a, PASP, 107, 156.

Holtzman, J.A., Burrows, C.J., Casertano, S., Hester, J.J., Trauger, J.T., Watson, A.M., & Worthey, G. 1995b, PASP, 107, 1065.

Hubble, E.P. 1936, "The Realm of the Nebulae", (New Haven: Yale Univ. Pr.).

Hunter, D.A., & Gallagher, J.S. 1986, PASP, 98, 5.

Hunter, D.A., Hawley, W.N., & Gallagher, J.S. 1993, AJ, 106, 1797.

Jimenez, R., Flynn, C., & Kotoneva, E. 1998, MNRAS, 299, 515.

Kingsburgh, R.L., & Barlow, M.J. 1995, A&AS, 295, 171.

Kudritzki, R. 1999, in the VLT Opening Symposium, Antofagasta, Chile, 1-4 March, 1999.

Lake, G.R., & Skillman, E.D. 1989, AJ, 98, 1274.

Landolt, A.U. 1992, AJ, 104, 340.

Langer, N. 1998, in IAU Symp. 190, "New Views of the Magellanic Clouds", Victoria, B.C., Canada, 12-17 July 1998, p. 17.

Langer, N., & Maeder, A. 1995, A&A, 295, 685.

Lavery, R.J., Seitzer, P., Walker, A.R., Suntzeff, N.B., & Da Costa, G.S. 1996, BAAS, 188, #09.03.

Lee, M.-G., Freedman, W.L., & Madore, B.F. 1993, ApJ, 417, 533.

Lee, Y.-W., Demarque, P., & Zinn, R. 1994, ApJ, 423, 248.

Marigo, P., & Girardi, L. 1998, in "New Views of the Magellanic Clouds", IAU Symp. 190, eds. Y.-H. Chu, N. Suntzeff, J. Hesser, & D. Bohlender, in press.

Marigo, P., Girardi, L., & Chiosi, C. 1996, A&A, 316, L1.

Mateo, M. 1998, ARA&A, 36, 435.

Minniti, D., & Zijlstra, A.A. 1996, AJ, 114, 147.

Mould, J.R., & Aaronson, M. 1982, ApJ, 263, 629.

Page, B.E.J., & Tautvaišienė, G. 1998, MNRAS, 299, 535.

Reid, I.N., & Mould, J.R. 1985, ApJ, 299, 236.

Reid, I.N., & Mould, J.R. 1990, ApJ, 360, 490.

Saha, A., Freedman, W.L., Hoessel, J.G., & Mossman, A.E. 1992, AJ, 104, 1072.

Saha, A., Labhardt, L., Schwengeler, H., Macchett, F.D., Panagia, N., Sandage, A., & Tammann, G.A. 1994, ApJ, 425, 14.

Sakai, S., Madore, B.F., & Freedman, W.L. 1996, ApJ, 461, 713.

Salpeter, E.E. 1955, ApJ, 121, 161.

Sandage, A.R. 1971a, ApJ, 166, 13.

Sandage, A.R., 1971b, in "Pontifica Academia Scientiarum Scripta Varia", ed. D.J.K. O'Connell (New York: Elsevier), p. 601.

Sandage, A.R., & Katem, B. 1976, AJ, 81, 743.

Schechter, P.L., Mateo, M., & Saha, A. 1993, PASP, 105, 1342.

Schlegel, D.J., Finkbeiner, D.P., & Davis, M. 1998, ApJ, 500, 525.

Seidel, E., Demarque, P., & Weinberg, D. 1987, ApJS, 63, 917.

Skillman, E.D. 1987, in Star Formation in Galaxies (Washington: NASA), p. 263.

Skillman, E.D., Kennicutt, R.C., & Hodge, P.W. 1989, ApJ, 347, 875.

Smecker-Hane, T.A., Stetson, P.B., Hesser, J.E., & Lehnert, M.D. 1994, AJ, 108, 507.

Stanek, K.Z., & Garnavich, P.M. 1998, ApJ, 503, 131.

Thuan, T.X., & Gunn, J.E. 1976, PASP, 88, 543.

Tolstoy, E. 1998, in "Dwarf Galaxies and Cosmology", XVIIth Moriond Astrophysics Meeting, eds. T.X. Thuan, C. Balkowski, V. Cayatte, J. Tran Thanh Van, in press, astro-ph/9807154.

Tolstoy, E. 1999, in "The Stellar Content of Local Group Galaxies", IAU Symp. 192, eds. P. Whitelock & R. Cannon, in press, astro-ph/9901245.

Tolstoy, E., Gallagher, J.S., Cole, A.A., Hoessel, J.G., Saha, A., Dohm-Palmer, R.C., Skillman, E.D., Mateo, M., & Hurley-Keller, D. 1998, AJ, 116, 1244.

Trumpler, R.J., & Weaver, H.F. 1953, "Statistical Astronomy", (Berkeley: Univ. Calif. Pr.), p. 392.

Udalski, A. 1998, AcA, 48, 383.

van den Bergh, S. 1967, AJ, 72, 70.

Wolf, M. 1907, MNRAS, 67, 91.